International Journal of Energetica (IJECA)
https://www.ijeca.info
ISSN: 2543-3717 Volume 7. Issue 1. 2022 Page 28-35

Switched Capacitor Nine-level inverter with reduced components for Grid connected PV systems using Fuzzy logic controller

H. Aboub[1*], R. Mechouma[1], B. Azoui[1]

[1]Dept. of Electrical Engineering, Laboratory LEB, University of Batna 2, Batna, ALGERIA

[*]Corresponding author E-mail: *haniaaboub @gmail.com*

Abstract – *The novel use of a three-phase switched capacitor SC nine-level inverter in a PV system is described in this article. It has a low input voltage, fewer components, and is grid-connected. The primary benefit of the suggested inverter is high voltage gain, which is attained by switching capacitors in series and parallel to raise the output voltage with the proper switching management. It is simpler to design a fuzzy logic controller to increase the infusion of solar energy into the electrical network. The MATLAB/Simulink environment's findings demonstrate that the suggested fuzzy logic controller performs well under a range of illumination levels. In comparison to the traditional PI controller, the total harmonic distortion (THD) obtained is less than the limit of 0.67 %. Good spectrum analysis and strong performance with fewer components are made possible by the nine-level SC inverter.*

Keywords: *Photovoltaic PV, Fuzzy logic controller FLC, Switched capacitor inverter SCI, Multi carriers SPWM , THD*

Received: 28/04/2022 – Revised 25/05/2022 – Accepted: 03/06/2022

I. Introduction

Because they provide effective ways to reduce pollution by using less fossil fuels, photovoltaic grid-connected systems have grown in importance across the globe [1-3]. Multilevel inverters have been acknowledged as a significant alternative to the typical two-level voltage source inverter [4], particularly in high PV power applications. These inverters can produce higher output voltages, which should be sinusoidal with lower switching frequency and lower total harmonic distortion [5,6].

Three categories—Neutral Point Clamped NPC, Flying Capacitor FC, and Cascaded H-Bridge Inverter—are used to classify common multilevel inverters in the literature [7,8]. An excessive number of diodes and unbalanced operation of DC-link's voltage divider capacitors are the major problems of NPC topology, [9-11]. Similar to this, the maximum output voltage of a flying capacitor multilayer inverter is equal to half of the DC input voltage.

The cascaded H-bridge multilevel converter topology, on the other hand, necessitates a separate DC source for each H-bridge [12], and a separate DC source for each phase compared to NPC and FC inverters [13]. Furthermore, all these multilevel inverters' topologies need more components and high input voltage PV sources in high voltage applications [14]. As a consequence, it is appropriate to improve the boost dc/dc converter with a higher conversion ratio or involve more numbers of PV cells in series [15].

Therefore, designing a particular topology for MLIs that has a less number of components and uses a lower DC voltage supply that is the switched-capacitor converter (SCC). This structure can be used as a multilevel converter coupled with conventional inverters to produce multi-level AC waveforms, or it can be utilized as a step-

up converter. Additionally, this inverter switches the capacitors in series and parallel by carefully choosing the switching control, resulting in output voltages that are higher than the input voltage. Moreover, many modulation techniques can be applied to drive a multilevel switched-capacitor inverter such as space vector modulation, Selected Harmonic Elimination (SHE), and Sinusoidal Pulse Width Modulation (SPWM). For the last decade, many types of research are conducted on the new topology of switched-capacitor inverters. A novel topology of a seven-level switched-capacitor inverter using the SPWM technique was presented. Also, a comparative study of seven-level switched-capacitor inverters using the same technique was applied for a very low input voltage. In addition, a Single Phase Five-Level switched capacitor Inverter for autonomous PV system applications without batteries has been implemented in a study [12], where the main objective is the test of a single phase nine-level switched-capacitor converter in low PV energy with a simple harmonic elimination technique. The authors also presented a Switched-Capacitor nine-level inverter with a modified hybrid modulation technique [16,17].
This paper aims to study a grid connected PV system based on a nine-level switched-capacitor inverter with SPWM technique controlled by a Fuzzy Logic controller. The remainder of the paper is organized as follows: the structure of a switched capacitor multilevel inverter is illustrated in section II. In section III, an explicit model control of the different sub-systems is described. Section IV shows a set of simulation results of the PV side. The results of the nine-level switched-capacitor inverter are discussed in this section. Finally, section V concludes this work.

II. Material and method

II.1. Proposed Switched capacitor nine level inverter Description

The proposed Switched-Capacitor Multilevel Inverter is seen in Figure 1 in its current configuration. It is created by cascading a Switched Capacitor Network and a two level (full bridge) inverter. This must first be converted to a high DC voltage before being converted to an Alternating Current.

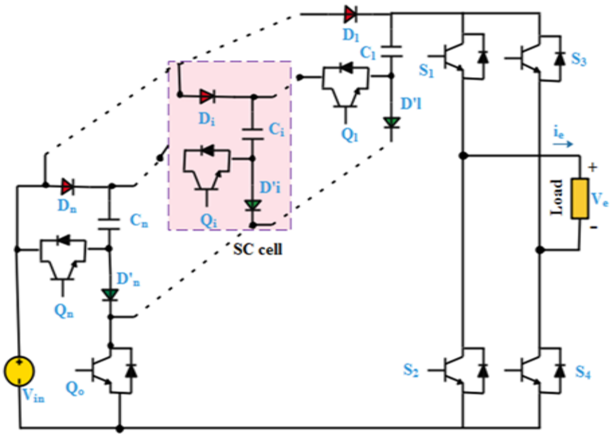

Figure 1. Topology of three phase Switched-Capacitor nine level inverter SCMLI

This topology can be used to get any number of levels with the help of series-parallel conversion operations. It consists of some Switched-Capacitor SC cells, each SC cell has one capacitor and two switches. Several output voltage levels can be obtained from one input voltage.
Therefore, assuming the number of capacitors is equal to n, the balanced voltage of each capacitor is to be provided by the equation that follows [14]:

$$V_{Ck} = 2^{k-1} V_{dc} \qquad \text{for k = 1, 2,.., n} \qquad (1)$$

Therefore, the maximum value of the output voltage ($V_{o.Max}$) and the number of generated output voltage levels (N_{-level}) are calculated with respect to n, using the following equations respectively:

$$V_{o.Max} = (\mathrm{n} + 1) * V_{dc} \qquad (2)$$

$$N_{level} = 2(n + 1) + 1 \qquad (3)$$

As a result, The switched capacitor nine-level inverter is composed of one voltage source from solar panels (Vpv), 3 diodes, 3 capacitors and 8 switches (power IGBT) [16,19]. The capacitors are charged when they are linked in parallel with the sources of the input voltage. The capacitors discharge when they are connected in series. The output voltage of nine level SCI can be four times higher than the input voltage.
Table 1 summarizes the switching states of various switches and capacitors for each mode in the proposed multilayer inverter.

Table 1. Switches and capacitors' States

V_{bus-DC}		V_{pv}	$2V_{pv}$	$3V_{pv}$	$4V_{pv}$
Capacitors states	C1	C	D	C	D
	C2	-	C	D	C
	C3	-	-	C	D
Switches states	S_1	1	1	0	1
	S_2	1	1	1	0
	S_3	0	1	0	0
	S_4	0	0	1	0
	S_5	0	0	0	1
	S_6	1	0	0	0
	S_7	0	1	0	0
	S_8	0	0	1	0

The letters C and D in Table 1 stand for the charging and discharging modes for capacitors, respectively, while the numbers 0 and 1 stand for the OFF and ON switching states. The following modes provide the expression for the output DC Bus voltage:

Mode 1: Capacitor C1 is charged to Vin when switch S6 is turned ON. This voltage level is concurrently transferred to the output by switches S1 and S2.
The expression of the output DC Bus voltage is:

$$V_{bus-DC} = V_{c1} = V_{in} \quad (4)$$

Mode 2: Through switch S7, the capacitor C2 is charged from Vin and voltage V_{c1} across the capacitor C1 (Capacitor C1 is gone discharged). The second level of the output DC Bus voltage is generated through S1, S2 and S3:

$$V_{bus-DC} = V_{in} + V_{c1} = 2 * V_{in} = V_{c2} \quad (5)$$

Mode 3: In this mode, the capacitor C3 is charged by Vin+Vc2 through switch S8 and the discharge of C2. Three voltage levels are concurrently created at the output through S1 and S3, and they equal 3Vin:

$$V_{bus-DC} = V_{in} + V_{c2} = 3 * V_{in} = V_{c3} \quad (6)$$

Mode 4: In this mode, Without adding another capacitor to the circuit, Switch S1 and S8 allow to transfer of the 4Vin voltage level into output by the stored voltage of C3 and the input voltage source as shown below [16]:

$$V_{bus-DC} = V_{in} + V_{c3} = 4 * V_{in} \quad (7)$$

It is important to note that, at this moment, C1is again charged directly by the DC voltage source for the next voltage level and this consecutive operation continues so on [20].

III. Results and analysis

III.1. Grid connected PV system design and modeling based on 9-level SCMLI topology

A DC/DC boost converter is used to extract the maximum power point by a fuzzy logic controller, and a DC-AC nine-level switched-capacitor inverter SCMLI can inject PV power into the grid with an RLC filter. Figure 2 shows the architecture of the proposed grid-connected PV system. It consists of a photovoltaic solar array of 5 kW for each phase, which is made up of five strings of 13 modules each. A fuzzy logic controller was utilized to regulate the current output pumped into the grid in order to control the switching patterns of the 9L-SCI.

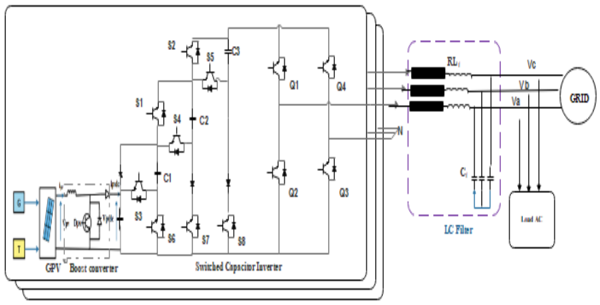

Figure 2. Architecture of grid connected PV system with three phase Switched-Capacitor nine level inverter SCMLI

Different components Models are shown as follows:
1- Under any condition, the photovoltaic module's (Ipv) current is provided by [21]:

$$I_{PV} = I_{ph} - I_{sa}\left[\exp\left[\frac{V_{pv}+R_s I_{pv}}{V_{th}}\right] - 1\right] - \frac{V_{pv}+R_s I_{PV}}{R_{SH}} \quad (8)$$

ui2-The boost converter is made up of two different Variables (IL, Vc).The model will be as follows:

$$\begin{bmatrix}\frac{di_L}{dt}\\ \frac{dv_c}{dt}\end{bmatrix} = \begin{bmatrix} 0 & -\frac{1-\alpha_{pv}}{L_{pv}} \\ \frac{1-\alpha_{pv}}{C} & -\frac{1}{RC}\end{bmatrix}\begin{bmatrix} i_{Lpv}\\ V_c\end{bmatrix} + [\tfrac{1}{L}\ 0]\begin{bmatrix}V_{pv}\\ 0\end{bmatrix} \quad (9)$$

3- In order to maximize the energy extracted from the PV array, a fuzzy logic control was used to generate the required cyclic ratio D of dc/dc boost converter corresponds to MPP for any change in temperature or irradiance.
4- The control of DC-link voltage:
In the present architecture, applying Kirchhoff current law at the DC-Link between the inverter and boost converter it yields

$$I_{dc} = C_{dc}\frac{dV_{dc}}{dt} = I_{out} - I_{inv}$$

Where:

- I_{out} is the boost output current known as I_{pv}
- I_{inv} is the input of inverter current: $I_{inv} = I_{grid} + I_{load}$
- C_{dc} is the DC-Link capacitor.

So:

$$\frac{dV_{dc}}{dt} = \frac{I_{pv} - I_{grid} - I_{load}}{C_{dc}}$$

In the present work, a fuzzy logic controller is proposed to regulate the DC link voltage of the PV interface system. The output of FLC gets the value of the reference network current.

5- To controller the three phase SC inverter, a virtual bi-phase system can be used, the d-q rotating frame is represented in the fallowing equations [22,23]:

$$\begin{cases} V_{gd} = V_{inv-d} - R_f I_{gd} - L_f \dfrac{dI_{gd}}{dt} + \omega_f L_f I_{gq} \\ V_{gq} = V_{inv-q} - R_f I_{gq} - L_f \dfrac{dI_{gq}}{dt} - \omega_f L_f I_{gd} \end{cases}$$

The expression of active and reactive power of grid can be represented by using the components of Park voltages after the filter and the currents of the grid [22,23]:

$$P = \frac{3}{2}(V_{gd}I_{gd} + V_{gq}I_{gq})$$

$$Q = \frac{3}{2}(V_{gq}I_{gd} - V_{gd}I_{gq})$$

6. Fuzzy Logic Control strategy of Nine-level switched-capacitor inverter :

Semiconductor devices must be turned ON and OFF in such a way that the desired fundamental is obtained with the least amount of harmonic distortion in order to synthesise a multilevel AC voltage output utilizing various levels of DC inputs. There are numerous methods for choosing switching methods for multilayer inverters. To produce n-level inverter output voltage, the SCMLI topology requires (n-1/2) carrier signals. It is based on a comparison between each carrier signal and a sinusoidal reference waveform. The active devices corresponding to that carrier are turned ON if the reference wave is greater than a carrier signal. If not, the gadgets are turned OFF. In order to create the gating pulses for each switch in the 9L-SCI control system, the control system produced four carrier signals and compared them to the reference voltage (Vref). In order to provide sinusoidal output, the output of this nine-level inverter is sent to the load and grid through an LC filter.

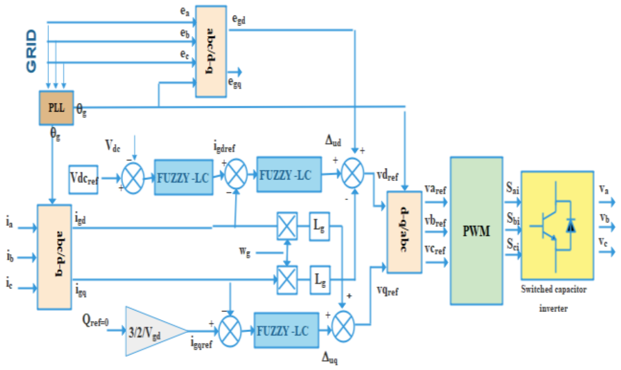

Figure 3. Block diagram for PWM with Fuzzy Logic Controller

The control circuit of the proposed inverter is shown in Figure 3. It is based on the use of FLC control in a closed loop The Fuzzy logic controller design is mainly involved three steps: Fuzzification, which allows the passage from the real domain to another fuzzy domain. The second block is devoted to the inference rules, while the last block is dedicated to the defuzzification part, to return to their al domain. This last operation uses the center of gravity, widely used, to determine the value of the control output. Both direct and quadratic currents grid fuzzy logic controller are shown in Figure 4.

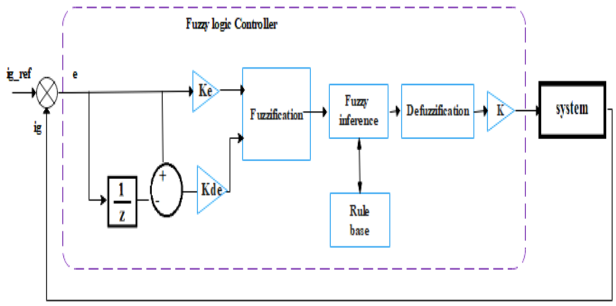

Figure 4. dq-axis current FL control scheme

$$\begin{cases} e_{id} = I^*_{gd} - I_{gd} \\ e_{iq} = I^*_{gq} - I_{gq} \end{cases} \quad (10)$$

At each instant, The controller FC produces the variation of Δu_d, Δu_q according to the difference between the two inputs **e** and Δ**e**, respectively:

$$\begin{cases} \Delta e_{id} = e_{id}(n) - e_{id}(n-1) \\ \Delta e_{iq} = e_{iq}(n) - e_{iq}(n-1) \end{cases} \quad (11)$$

Where:

-The current I^*_{gd} is generated also by a Fuzzy Logic controller according to the produced PV power.

-The current the I^*_{gq} is estimated in term of reactive power reference using the following equation:

$$I_{gq\_ref} = \frac{2Q_{g\_ref}}{3V_{gd}}$$

III.2. Simulation of the overall system

This section displays the various simulation results that were obtained using the MATLAB/Simulink environment. The intensity of sunlight is considered to be varied between 500 and 1000 W/m^2 as shown in Figure 5, and variation in the load power is shown in Figures 6 to Figure 16 supporting the performance of the fuzzy logic controller on the AC side.

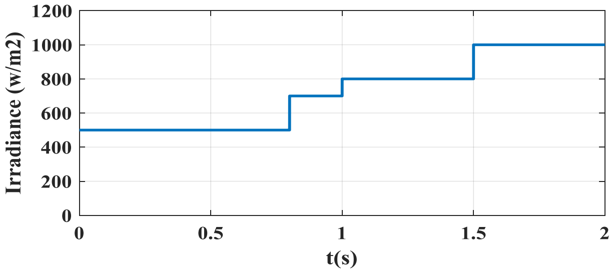

Figure 5. Variation of irradiation Levels

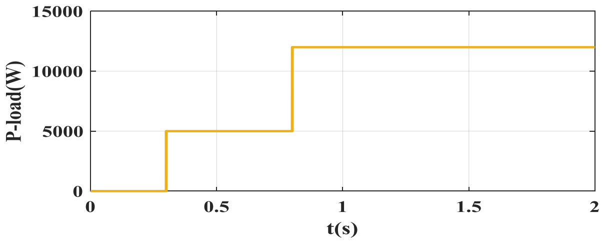

Figure 6. Power of Load power

The results of simulations of the overall system is shown in following figures:

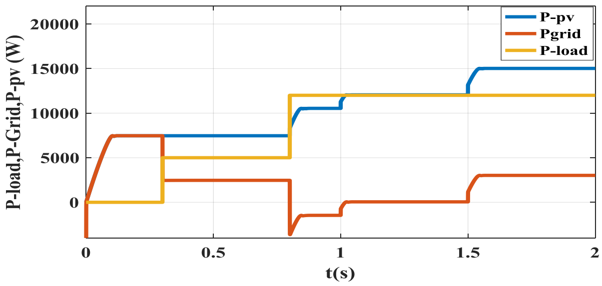

Figure 7. Power of Load power

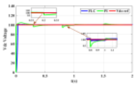

Figure 8. Input voltage of Nine-level SCI

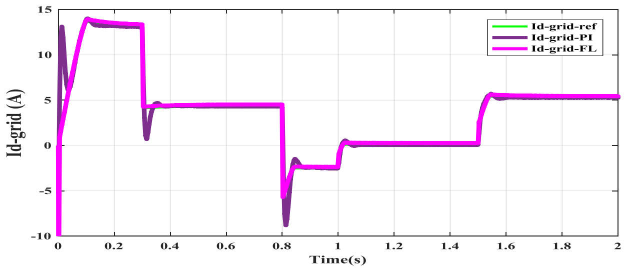

Figure 9. Comparison of direct current grid of FLC and PIC

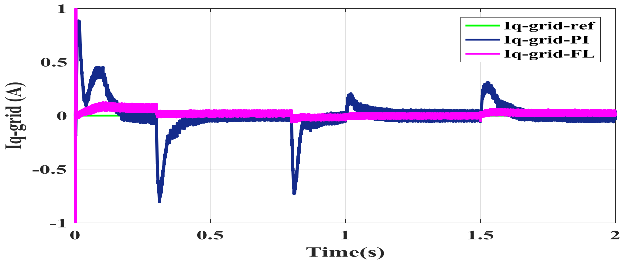

Figure 10. Quadratic grid current of FLC

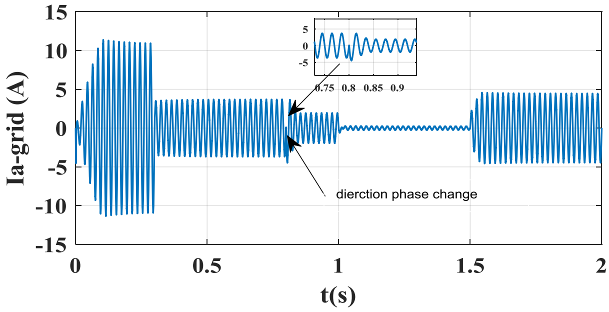

Figure11. Grid current of phase a with FLC

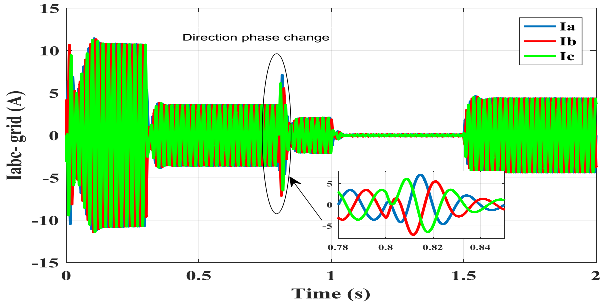

Figure 12. Three phase grid current

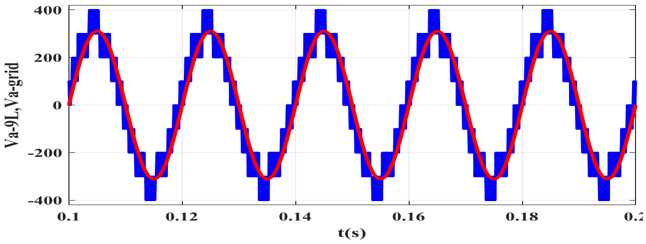

Figure 13. Output voltage of 9 L Switched capacitor inverter

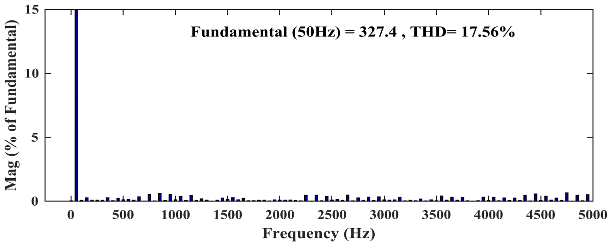

(a)

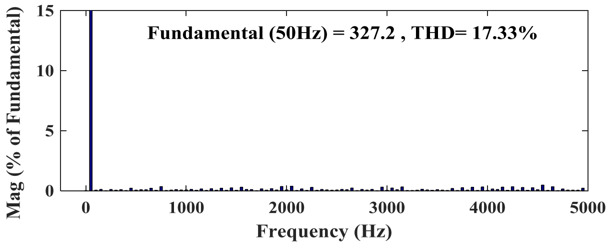

(b)

Figure 14. Nine-level SC inverter FFT analysis of the voltage of the phase "a(a): with PI controller and (b): with FL controller

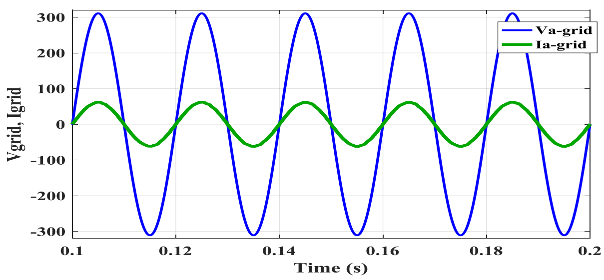

Figure 15. Voltage and current grid of phase a

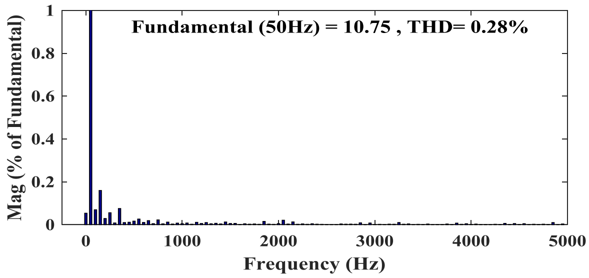

(a)

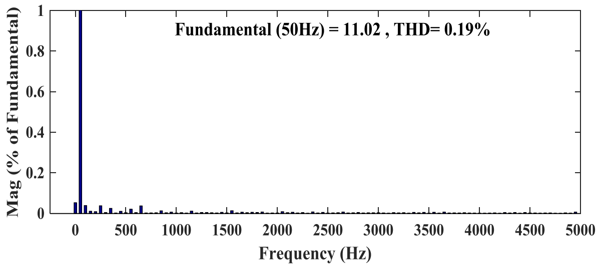

(b)

Figure 16. FFT analysis of the grid current : (a): with PI controller and (b): with FL controller

III.3. Discussions of the results

During the first interval [0 à 0.3], the all generated PV power injected to the grid, at 0.3s occurs the first step change in the load power from 0 to 5Kw, this change leads to a small undershoot in Vdc over its reference with FLC compared with PI controller as shown in Figure 8.

At 0.8s an increase in the load demand is greater than the energy produced by the photovoltaic generator. In this case, the surplus of the power load from the electrical network is covered as observed in Figures 7 and 9. The phase change at this moment is visible as seen in Figures 11 and 12 since the grid current reflects its direction.

There is no energy sent to the network because it can be seen at the field between 1 and 1.5 that the energy generated equals the energy needed for the load. As a result, the electrical network's current in this entire field is practically zero.

In addition, it can be noted in Figures 9 and 10 that FLC always gives a better result than the PI for any change, whether in irradiance of the sun or the power load. Also Figures 15 and 16 show that the current grid with PI controller has a sinusoidal waveform with 0.28 THD per cent for current, this result can be reduced by using the FL controller to 0.19%.

Furthermore, it can be noted in Figures 13 and 14 that the voltage of output 9L-SCI has a waveform stairway shape with a peak value of 400V= 4*Vin. The Fast Fourier transform (FFT) analysis gives an acceptable value of THD.

IV. Conclusion

Nine level switched-capacitor inverter 9LSCI was proposed to inject PV power into the grid.

- This inverter can produce a high gain voltage which is increasing four times the output voltage by using low voltage input (100 V) with a minimum number of components.
- The efficiency of the fuzzy logic controller is very satisfying with a reduced number of harmonic of 0.67% in efficiency obtained while compared to the classic PI controllers, and it achieves high quality outputs, and low THD an improvement.

Declaration

- The authors declare that they have no known financial or non-financial competing interests in any material discussed in this paper.
- The authors declare that this article has not been published before and is not in the process of being published in any other journal.
- The authors confirmed that the paper was free of plagiarism.

References

[1] M. Rabiaa, A. Hania, A. Boubakeur, "Multicarrier wave dual reference very low frequency PWM control of a nine levels NPC multistring three phase inverter topology for photovoltaic system connected to the medium electric grid, " J. Electr. Eng, Vol. 16, No. 2, pp. 293–8, 2020. DOI: 10.1109/UPEC.2014.6934666

[2] H. Aboub, R. Mechouma, B. Azoui, C. Labiod, A. Khechekhouche, "A New Multicarrier Sinusoidal Pulse Width Modulation (SPWM) Strategy based on Rooted Tree Optimization (RTO) Algorithm for Reducing Total Harmonic Distortion (THD) of Switched-Capacitor Nine-level Inverter in Grid-connected PV systems," Indonesian Journal of Science & Technology, vol 7, no 1, 2021. https://doi.org/10.17509/ijost.v7i1.41716

[3] A. Nouaiti, A. Saad, A. Mesbahi, M. Khafallah, "Implementation of a Single Phase Switched-Capacitor Nine-Level Inverter for PV System Applications with Selective Harmonic Elimination," Int. J. Comput. Appl, Vol. 168, No.7, pp. 9–15, 2017. 10.5120/ijca2017914416.

[4] M.A. Husain, A. Tariq, S. Hameed, M.S. Bin Arif, A. Jain, "Comparative assessment of maximum power point tracking procedures for photovoltaic systems, " Green Energy Environ, Vol. 2, No.1, pp. 5–17, 2017. 10.1016/j.gee.2016.11.001.

[5] M. Derakhshanfar, "Analysis of different topologies of multilevel inverters," International Journal of Engineering Research & Technology (IJERT), Vol. 2, No. 9, pp. 304–9, 2010.

[6] K. Oliveira, J. Afonso, M. Cavalcanti, K. Oliveira, J. Afonso, M. Cavalcanti, M. Inverter, F. Function, S. Tomic, "Multilevel Inverter for Grid-Connected Photovoltaic Systems with Active Filtering Function To cite this version : HAL Id : hal-01348766 Multilevel Inverter for Grid-connected Photovoltaic Systems with Active Filtering Function, " International Journal of Engineering Research & Technology (IJERT), Vol. 6, No. 05, pp. 752-758, 2016. http://dx.doi.org/10.17577/IJERTV6IS050454.

[7] P. Pany, R.K. Singh, R.K. Tripathi, "Performance analysis of fuel cell and battery fed PMSM drive for electric vehicle application, " ICPCES 2012 - 2012 2nd Int. Conf. Power, Control Embed. Syst, 2012. 10.1109/ICPCES.2012.6508118.

[8] J. Rocabert, J. Crébier, J. Peracaula, J. Rocabert, J. Crébier, J.P. "Diode-clamped, Diode-clamped multilevel converters with integrable gate-driver power-supply circuits," To cite this version : HAL Id : hal-00422539 Diode-Clamped Multilevel Converters with Integrable, 2009. https://hal.archives-ouvertes.fr/hal-00422539

[9] Sharifzadeh, Mahdi, Alexandra Sikinioti-Lock and Nilay Shah. "Machine-learning methods for integrated renewable power generation: A comparative study of artificial neural networks, support vector regression, and Gaussian Process Regression" Renewable and Sustainable Energy Reviews, Vol. 108, pp. 513–38, 2019. 10.1016/j.rser.2019.03.040.

[10] S.R. Teja, P.U. Sankar, Y. Rajkumar, "Switched Capacitor Seven-level Inverter," International Journal of Pure and Applied Mathematics, Vol.114, No.12, pp. 535–43, 2017.

[11] Y. Hinago, H. Koizumi, "A switched-capacitor inverter using series/parallel conversion with inductive load," IEEE Trans. Ind. Electron, Vol. 59, No 2, pp. 878–87, 2012. 10.1109/TIE.2011.2158768.

[12] A. Nouaiti, A. Saad, A. Mesbahi, M. Khafallah, "Experimental Implementation of a Low-Cost Single Phase Five-Level Inverter for Autonomous PV System Applications Without Batteries," Eng. Technol. Appl. Sci. Res. Vol. 8, No 1, pp. 2452–2458, 2012. DOI: 10.48084/etasr.1675

[13] M. Baldé, M.L. Doumbia, A. Chériti, C. Benachaiba, "Comparative study of NPC and Cascaded converters topologies," Renew. Energy Power Qual. J. Vol. 1, No 9, pp. 185–190, 2011. 10.24084/repqj09.282.

[14] P.S. Bhagyalakshmi, B.M. Varghese, J. Joy, "Inverters Using Sinusoidal Multicarrier PWM Technique," International Journal of Advanced Research in Electrical, Electronics and Instrumentation Engineering, Vol. 5, No 10, pp. 8145–8154, 2016. 10.15662/IJAREEIE.2016.0510053.

[15] B. Yang,, W. Li, Y. Gu, W. Cui, X. He, " Improved transformerless inverter with common-mode leakage current elimination for a photovoltaic grid-connected

power system," IEEE Trans. Power Electron, Vol. 27, No 2, pp. 752–762, 2012. 10.1109/TPEL.2011.2160359.

[16] H.N. Avanaki, R. Barzegarkhoo, E. Zamiri, "A Switched-Capacitor Multilevel Inverter for grid-connected PV systems with MPPT ability and reduced components," 9th Annu. Int. Power Electron. Drive Syst. Technol. Conf. PEDSTC, pp. 224–230, 2018. 10.1109/PEDSTC.2018.8343800.

[17] E. Zamiri, R. Barzegarkhoo, B. Karami, S.H. Hosseini, "A hybrid switched-capacitor multilevel inverter with self charge balancing and less number of switches," 6th Annu. Int. Power Electron. Drive Syst. Technol. Conf. PEDSTC, pp. 573–578, 2015. 10.1109/PEDSTC.2015.7093338.

[18] B. Karami, R. Barzegarkhoo, A. Abrishamifar, M. Samizadeh, " A switched-capacitor multilevel inverter for high AC power systems with reduced ripple loss using SPWM technique," 6th Annu. Int. Power Electron. Drive Syst. Technol. Conf. PEDSTC, pp. 627–632, 2015. 10.1109/PEDSTC.2015.7093347.

[19] N. Sandeep, U.R. Yaragatti, "A Switched-Capacitor-Based Multilevel Inverter Topology with Reduced Components," IEEE Trans. Power Electron, Vol. 33, No. 7, 2018. 10.1109/TPEL.2017.2779822.

[20] M. Saeedian, E. Pouresmaeil, E. Samadaei, E.M. Godinho Rodrigues, R. Godina, M. Marzband, "An innovative dual-boost nine-level inverter with low-voltage rating switches," Energies, Vol. 12, No. 2, pp. 1–15, 2019. 10.3390/en12020207.

[21] M. Maamir, O. Charrouf, A. Betka, M. Sellali, M. Becherif, "Neural network power management for hybrid electric elevator application," Math. Comput. Simul, Vol. 167, pp. 155–175, 2020 https://doi.org/10.1016/j.matcom.2019.09.008

[22] M. Kermadi, Z. Salam, E.M. Berkouk, "An adaptive sliding mode control technique applied in grid-connected PV system with reduced chattering effect," IEEE Conf. Energy Conversion, CENCON, pp.180–185, 2017. DOI: 10.1109/CENCON.2017.8262480

[23] U. Yilmaz, A. Kircay, S. Borekci, "PV system fuzzy logic MPPT method and PI control as a charge controller," Renew. Sustain. Energy Rev. Vol. 81, pp. 994–1001, 2018. https://doi.org/10.1016/j.rser.2017.08.048